

Measurement of Coherent Transition X Rays

M. J. Moran, B. A. Dahling, and P. J. Ebert

Lawrence Livermore National Laboratory, University of California, Livermore, California 94550

M. A. Piestrup

Adelphi Technology, Woodside, California 94062

B. L. Berman

Department of Physics, The George Washington University, Washington, D.C. 20052

and

J. O. Kephart

Department of Electrical Engineering, Stanford University, Stanford, California 94305

(Received 16 June 1986)

We have observed coherent multiple-foil transition radiation in the x-ray energy region.

PACS numbers: 41.70.+t, 07.85.+n, 34.80.-i

In a previous Letter,¹ we reported the observation of *intrafoil* coherence of transition radiation in both the angular distribution and the absolute intensity of soft x rays produced by 25-MeV electrons incident on a target consisting of eighteen 1- μm -thick Be foils. In this Letter, we report evidence of *interfoil* coherence.

The experimental apparatus has been described previously.^{1,2} We obtained the present results with 54-MeV electrons perpendicularly incident on targets of polypropylene foils. X-ray angular distributions and spectra were measured with a thin-window flow proportional counter. This counter used a mixture of 90% neon and 10% isobutane at a pressure of 200 Torr. The x-ray spectra were corrected for absorption in the 28- $\mu\text{g}/\text{cm}^2$ -thick VYNS counter window. For low-energy photons, the energy resolution was relatively poor, varying from 50% at 300 eV to $\sim 100\%$ at 50 eV. Therefore, the angular distribution measurements, which had an angular resolution of 1 mrad, were integrated over an energy range that was comparable to the measured photon energy.

The polypropylene foils were stretched to a thickness of $0.55 \pm 0.06 \mu\text{m}$. Their thickness was gauged by comparison with the characteristic colors of transparent foils with thicknesses in this range.³ The thickness also was determined by the weighing of foils of known area and use of a bulk density of $0.91 \text{ g}/\text{cm}^3$. These techniques gave results that were consistent with the total carbon content of the foils as determined by Rutherford backscattering of protons and alpha particles. We used three different two-foil targets, which had spacings of 3000, 100, and $50 \mu\text{m}$. The foils were mounted on 1-cm-square silicon frames 50 or $100 \mu\text{m}$ thick. Those foils then were stacked to achieve the desired spacing. A fourth target consisted of four foils

with $100\text{-}\mu\text{m}$ spacers.

Figure 1 shows the measured angular distributions and spectra. For all cases, the backgrounds were low and have been subtracted.^{1,2} Figure 1(a) shows data for the two-foil target with $3000\text{-}\mu\text{m}$ spacing. The dots represent the experimental data, and the solid curve was obtained by the averaging of neighboring points. Figure 1(e) shows the spectra measured at the angles indicated in Fig. 1(a). These data are similar to the single-foil angular distributions and spectra reported previously.^{1,2} The angular resolution was incapable of resolving the interfoil interference that is characteristic of this spacing (see below).

Figures 1(b)–1(d) show the angular distributions recorded for two-foil targets with $50\text{-}\mu\text{m}$ and $100\text{-}\mu\text{m}$ spacings and for the four-foil target with $100\text{-}\mu\text{m}$ spacing, respectively. The solid curve is the same one shown in Fig. 1(a). Figures 1(f)–1(h) show the corresponding spectra at the angles indicated. The angular distributions for these targets show maxima and minima that are characteristic of interference phenomena, and the distributions differ from target to target. Most of the energy spectra are dominated by a broad peak near 150 eV. This peak is characteristic of $0.55\text{-}\mu\text{m}$ -thick polypropylene foils. However, the destructive interference at the valleys in the angular distributions (e.g., cases 5 and 9 shown in Fig. 1) is manifested by the absence of the 150-eV peak in the corresponding spectra.

The angular distributions in Figs. 1(b)–1(d) indicate strong interference of the 150-eV photons (wavelength $\approx 83 \text{ \AA}$) generated in the closely spaced foils. Photons of this wavelength interfere in the targets because relativistic contraction (for 54-MeV electrons) reduces the effective foil spacing by a factor of $\approx 10^4$.

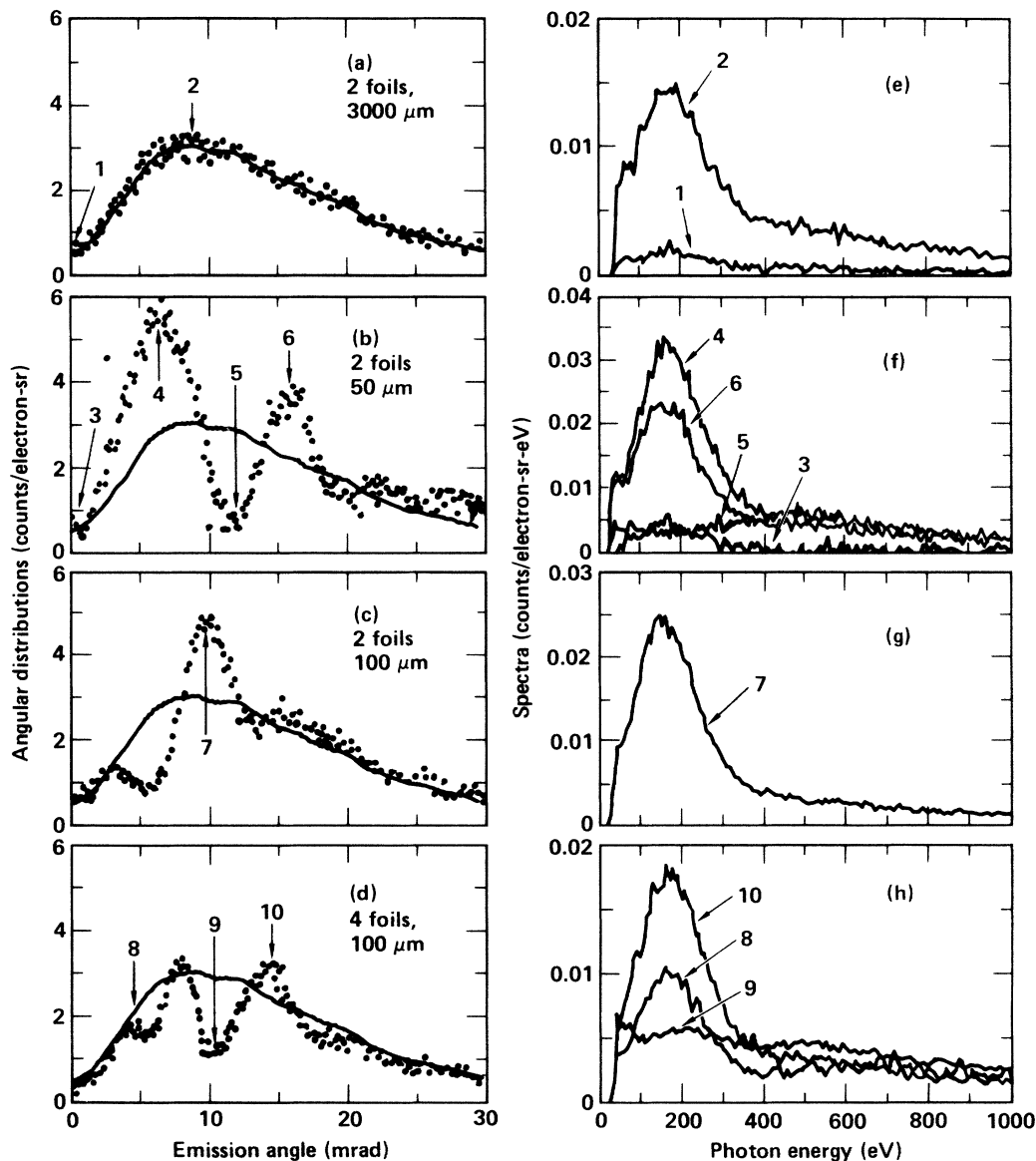


FIG. 1. (a)–(d) Angular distributions and (e)–(h) energy spectra for transition radiation from 54-MeV electrons traversing polypropylene foil targets.

This interference behavior demonstrates that the transition x rays are generated coherently by the entire target structure. “Coherent,” in this case, refers to the fact that transition-photon generation is a simultaneous response of the entire target structure to each incident electron. The measurements were conducted at low intensities (the average current was $\leq 10^{-1}$ A) so that usually there was no more than a single electron traversing the target at a given time, and therefore the generation of more than a single photon at any given time was very rare. Thus, no photon can be identified as having been generated at any single surface in the target. This behavior is similar to that in a

multiple-slit photon-diffraction experiment at low light intensity. The present case is unusual because the foil spacings are $\approx 10^4$ times greater than the photon wavelength of interest. Thus, our results demonstrate the relativistic contraction mentioned above. The results also are consistent with similar data for visible photons for two-surface interference of transition radiation that have been reported previously.⁴

A quantitative description of transition radiation generated by a multiple-foil target can be calculated with the following simplified form¹

$$d^2N(\omega, \theta)/d\omega d\Omega = N_0 F_f F_M, \quad (1)$$

where $N(\omega, \theta)$ is the number of photons, ω is the radial frequency of the radiation, Ω is the solid angle, and θ is the angle of emission. In Eq. (1), N_0 describes the radiation generated at a single vacuum-material interface and can be written in the form^{1,2}

$$N_0 = (\alpha \omega \sin^2 \theta / 16 \pi^2 c^2) (Z_1 - Z_2)^2, \quad (2)$$

where α is the fine-structure constant ($\alpha \approx \frac{1}{137}$), c is the speed of light, and Z_1 and Z_2 are the "formation lengths" in vacuum and in the foil medium, respectively. The Z_i are given by

$$Z_i = 4(c/\omega) \beta [(1/\gamma)^2 + (\omega_i/\omega)^2 + \theta^2]^{-1}, \quad (3)$$

where γ is the electron energy divided by its rest energy, β is v/c , v is the electron speed, and ω_i is the relevant electron plasma frequency when the dielectric constant $\epsilon_i(\omega)$ of the medium is given by the Drude free-electron theory as⁵

$$\epsilon_i(\omega) \approx 1 - (\omega_i/\omega)^2. \quad (4)$$

The factor F_f describes the coherent addition of photons generated at the two surfaces of a single foil and can be written in the form

$$F_f = 1 + \exp(-\sigma_2) - 2 \exp(-\sigma_2/2) \cos(2l_2/Z_2), \quad (5)$$

where $\sigma_2 = \mu_2 l_2$, μ_2 is the x-ray absorption coefficient of the foil material and l_2 is the foil thickness.⁶ The form for F_f in Eq. (5) differs from the one in our previous publications because the present form accounts as well for x-ray absorption in the single foil.^{1,2}

The factor F_M describes the coherent addition of photons generated by the multiple foils in a target, and for our present purposes can be written as

$$F_M = \frac{1 + \exp(-M\sigma_2) - 2 \exp(-\frac{1}{2}M\sigma_2) \cos(2MX)}{1 + \exp(-\sigma_2) - 2 \exp(-\frac{1}{2}\sigma_2) \cos(2X)}, \quad (6)$$

where M is the number of foils in the target, $X = l_1/Z_1 + l_2/Z_2$, and l_1 is the foil separation. In our previous experiments, where interfoil interference effects were not resolvable, Eq. (1) accurately predicted the measured transition radiation for a wide range of photon energies and angles of emission, for a number of different foil materials.^{1,2}

In the present experiment we have clearly resolved interference behavior in the angular distribution of transition radiation. Figure 2 compares the measured and calculated angular distributions. The calculations use the measured electron energy, foil thickness, and spacing with the above equations. The spectra are integrated from 50 to 300 eV and are corrected for varia-

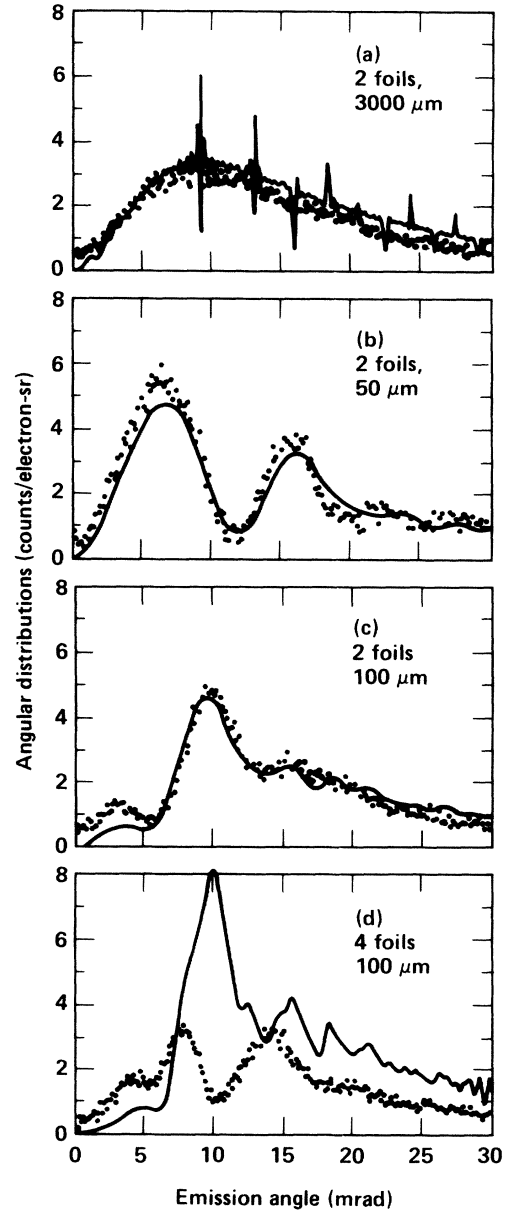


FIG. 2. Measured (data points) and calculated (curves) angular distributions for transition radiation from 54-MeV electrons traversing polypropylene foil targets.

tions in detector efficiency. The calculated results are sensitive to the value taken for the electron plasma frequency of the foil material, ω_2 . The calculated curves shown in Fig. 2 assume a value for ω_2 that is 1.05 times the nominal value; use of the nominal value for ω_2 results in a poorer fit.

The sharp structure in the calculated curve of Fig. 2(a) represents interference phenomena for the target with 3000- μm spacing, but is not apparent in the data because of the limited angular resolution of the detector. The calculated angular distributions in Figs. 2(b) and 2(c) for the closely spaced two-foil targets show

excellent agreement with the measurements. However, the calculated curve for the four-foil target shown in Fig. 2(d) differs markedly from the measured data. There are several possible reasons for this disagreement, but the most likely is that the foil-to-foil spacing is not uniform throughout the target.

These measurements constitute the basis of a new technique for the measurement of soft x-ray dielectric constants. For the parameters of interest here, the resonance behavior is strongly dependent upon the formation length, which in turn is highly sensitive to the dielectric constant. Since the interference behavior is determined largely by the magnitude of l_2/Z_2 , angular distributions measured for specific photon energies can determine the associated dielectric constant by use of the functional dependence of Z_2 on the dielectric constant.⁷

In summary, we have observed interference phenomena in the angular distributions and spectra of transition radiation from closely spaced two- and four-foil polypropylene targets. Strong interference occurred for photons having wavelengths of $\approx 83 \text{ \AA}$. Calculated angular distributions are in excellent agreement with the two-foil data. These results form the basis of a new technique for measuring x-ray dielectric constants.

The authors thank R. H. Pantell for the loan of electronic equipment, P. Calavan for improvements in the

experimental apparatus, S. Shiromizu for supplying the polypropylene foils, D. Ciarlo and J. Trevino for target fabrication, and R. Musket for Rutherford-scattering thickness measurements. This work was performed at the Lawrence Livermore National Laboratory under the auspices of the U.S. Department of Energy under Contract No. W-7405-Eng-48.

¹P. J. Ebert, M. J. Moran, B. A. Dahling, B. L. Berman, M. A. Piestrup, J. O. Kephart, H. Park, R. K. Klein, and R. H. Pantell, *Phys. Rev. Lett.* **54**, 893 (1985).

²M. A. Piestrup, J. O. Kephart, H. Park, R. K. Klein, R. H. Pantell, P. J. Ebert, M. J. Moran, B. A. Dahling, and B. L. Berman, *Phys. Rev. A* **32**, 917 (1985).

³M. Francon, in *Handbuch der Physik*, edited by S. Flugge (Springer-Verlag, Berlin, 1956), Vol. 24, p. 207.

⁴L. Wartski, S. Roland, J. LaSalle, M. Bolore, and G. Filippi, *J. Appl. Phys.* **46**, 3644 (1975).

⁵P. K. L. Drude, *Theory of Optics* (Dover, New York, 1959).

⁶X-ray absorption cross sections were taken from E. F. Plechaty, D. E. Cullen, and R. J. Howerton, Lawrence Livermore National Laboratory Report No. UCRL-50400, Vol. 6, Rev. 3, 1981 (unpublished).

⁷X. Artru, G. B. Yodh, and G. Mennessier, *Phys. Rev. D* **12**, 1289 (1975).